

The Magnetism of Li doped La_2CuO_4 : the antiferromagnetic spin-shard state

O. P. Sushkov¹ and A. H. Castro Neto²

¹*School of Physics, University of New South Wales, Sydney 2052, Australia*

²*Department of Physics, Boston University, 590 Commonwealth Avenue, Boston, Massachusetts 02215, USA*

(Dated: November 12, 2018)

We study the dynamics of a single hole in Li and Sr doped La_2CuO_4 and its extension to a finite hole concentration. We compare the physics of $\text{La}_{2-x}\text{Sr}_x\text{CuO}_4$ and $\text{La}_2\text{Cu}_{1-x}\text{Li}_x\text{O}_4$ and explain why these systems are remarkably different. We demonstrate that holes in $\text{La}_2\text{Cu}_{1-x}\text{Li}_x\text{O}_4$ are always localized and that there is a critical concentration, $x_c \approx 0.03$, above which the holes break the global antiferromagnetic state into an array of weakly coupled antiferromagnetic clusters (antiferromagnetic shards). We show that the spin-shard state provides a description of the magnetic and electric properties of $\text{La}_2\text{Cu}_{1-x}\text{Li}_x\text{O}_4$. Two experiments that can test our theory are proposed.

PACS numbers: 74.72.Dn, 75.10.Jm, 75.30.Fv, 75.50.Ee

Introduction. The sharp contrast in the physical properties of Sr and Zn doping in La_2CuO_4 is not surprising since Sr brings mobile holes into the CuO_2 planes while Zn does not. At the same time the remarkable differences between Li and Sr doping of La_2CuO_4 are somewhat surprising since both Sr and Li ions bring mobile holes into CuO_2 planes. It is by now well established that $\text{La}_{2-x}\text{Sr}_x\text{CuO}_4$ (LSCO) and $\text{La}_2\text{Cu}_{1-x}\text{Li}_x\text{O}_4$ (LCLiO) have very different physical properties: LSCO has an insulator-superconductor transition at $x \approx 0.055$ [1] while LCLiO remains an insulator at all dopings [2]. Elastic and inelastic neutron scattering in LSCO at $x > 0.02$ reveals incommensurate magnetic peaks [3, 4, 5, 6] while neutron scattering in LCLiO is always commensurate [7, 8, 9] with a very unusual scaling behavior of the magnetic response [8, 9]. There is, however, a similarity between these compounds: the long-range Néel order is destroyed at rather close values of doping, $x = 0.02$ in LSCO and $x = 0.03$ in LCLiO [1, 10].

It is clear that the origin of the differences between Sr and Li doping is in the fact that Sr substitutes La ions outside of the CuO_2 planes while Li ions substitute in plane for Cu ions. Every dopant injects a hole into the plane, but the Sr ion seems to be a relatively weak hole scatterer while the Li ion interacts strongly with the injected holes. To understand the differences between these two systems we first consider the problem of an impurity bound state formation in a strongly correlated CuO_2 plane. Then we generalize our solution for a finite concentration of holes and find that there is a critical concentration x_c above which a spin-shard state is formed. We show that the formation of this state can explain the observed properties of LCLiO.

Coulomb trapping of a single hole. The problem of a single hole trapped by a Sr ion has been solved recently in Ref. [11]. In this work we extend that solution to the case of Li doping. Similarly to the case studied in Ref. [11] we perform the analysis within the $t-t'-t''-J$ model that is assumed to describe the low energy, $\epsilon \leq 4t \sim 1\text{eV}$, dynamics of CuO_2 planes. The parameters of the effective

$t-t'-t''-J$ model are well known: from the Raman scattering studies [12] it was found that $J \approx 125\text{ meV}$; following the calculations of Andersen *et al.* [13] we set $t/J = 3.1$, $t'/J \approx -0.5$, and $t''/J \approx 0.3$. We measure the energy in units of J , length in units of the lattice spacing a , and set $\hbar = 1 = k_B$. The kinetic terms t' and t'' are small compared to t and our results for LCLiO are not *qualitatively* sensitive to their precise values [14]. Nevertheless, these matrix elements are quantitatively important because they describe hopping within the same magnetic sublattice and influence the hole dispersion.

Because of the strongly interacting environment where the hole moves, the hole dynamics is strongly dressed by quantum spin fluctuations with momenta $\mathbf{q} \sim (\pi, \pi)$. This dressing leads to the effective hole (quasihole or small magnetic polaron) that describes dynamics of the system at even lower energies, $\epsilon \leq J$. This part of the problem is well understood and is independent of the presence of the impurity. In momentum space, the minima of the quasihole dispersion appear near $\mathbf{k}_0 = (\pm\pi/2, \pm\pi/2)$, which are the centers of the four faces of the reduced magnetic Brillouin zone (MBZ). In vicinity of these points the dispersion is quadratic: $\epsilon_{\mathbf{k}} \approx \beta_1 k_1^2/2 + \beta_2 k_2^2/2$, where \mathbf{k} is defined with respect to \mathbf{k}_0 , \mathbf{k}_1 is perpendicular to the face of the MBZ, while \mathbf{k}_2 is parallel to it. In the self-consistent Born approximation [15] the hole dispersion is isotropic, $\beta_1 \approx \beta_2 = \beta \approx 2.2$, and has a finite quasiparticle residue, $Z \approx 0.34$.

In the presence of a negatively charged impurity, the hole is trapped near the impurity ion by the Coulomb potential $-e^2/(\epsilon_e \sqrt{r^2 + d^2})$, where $\epsilon_e \sim 30 - 100$ is the effective dielectric constant of La_2CuO_4 [1], and d is the distance of the ion from the CuO_2 plane. In the cases discussed here we can set $d = 0$ since its effect is rather small. The most important difference between the Li and the Sr doping is that the hole cannot penetrate on the Li site because of a strong hard core repulsion. Thus, we can model the potentials for Sr and Li as:

$$\text{Sr} : V(r) = -\frac{e^2}{\epsilon_e r}, \quad \text{Li} : V(r) = -\frac{e^2}{\epsilon_e r} + G\delta(\mathbf{r}),$$

where G is a very large positive constant. The δ -function term in the Li potential enforces a node of the bound-state wave function at the origin. So the ground state wave function in the Li case can have either s-wave with a node, or p-wave symmetry.

Because of the presence of the bound state the local magnetic configuration relaxes, leading to the formation of a spin texture: the spin at every site can rotate by an angle θ_i with respect to the orientation at $r = \infty$. There are two sublattices, “up” and “down”, so that:

$$\begin{aligned} |i\rangle &= e^{i\theta(\mathbf{r}_i)\mathbf{m}\cdot\boldsymbol{\sigma}/2} |\uparrow\rangle, \quad i \in \text{“up” sublattice}, \\ |j\rangle &= e^{i\theta(\mathbf{r}_j)\mathbf{m}\cdot\boldsymbol{\sigma}/2} |\downarrow\rangle, \quad j \in \text{“down” sublattice}. \end{aligned}$$

Here $\mathbf{m} = (\cos\alpha, \sin\alpha, 0)$ with arbitrary α is the “director” of the state. The director is orthogonal to the magnetization plane. Note that the directions in spin space are completely independent of directions in coordinate space. Because of the sublattice structure, the wave function of the hole $\psi(\mathbf{r})$ has two components, pseudospin up and pseudospin down, corresponding to a hole moving in the up and down sublattices, respectively. The total energy is of the form [15, 16]:

$$E = \int d^2r \left\{ \frac{\rho_s}{2} (\nabla\theta)^2 + \psi^\dagger(\mathbf{r}) \begin{pmatrix} -\beta\frac{\nabla^2}{2} - \frac{e^2}{\epsilon_e r} & \sqrt{2}ge^{-i\alpha}(\mathbf{e}\cdot\nabla\theta) \\ \sqrt{2}ge^{i\alpha}(\mathbf{e}\cdot\nabla\theta) & -\beta\frac{\nabla^2}{2} - \frac{e^2}{\epsilon_e r} \end{pmatrix} \psi(\mathbf{r}) \right\}, \quad (1)$$

where $\rho_s/J \approx 0.18$ is the spin stiffness of environment and \mathbf{e} is a unit vector orthogonal to a given face of the MBZ. If the hole “resides” in the pocket near $\mathbf{k}_0 = (\pi/2, \pi/2)$ then $\mathbf{e} = (1/\sqrt{2}, 1/\sqrt{2})$, and if the hole “resides” in the pocket near $\mathbf{k}_0 = (\pi/2, -\pi/2)$ then $\mathbf{e} = (1/\sqrt{2}, -1/\sqrt{2})$. There is coupling between different pockets, but this is an exponentially small effect and can be safely neglected. Finally, $g = Zt \approx 1.05$ is the effective hole-spin-wave coupling constant. The solution of (1) is of the form

$$\psi(\mathbf{r}) = \frac{1}{\sqrt{2}} \begin{pmatrix} 1 \\ -e^{i\alpha} \end{pmatrix} \chi(r), \quad (2)$$

where,

$$\text{Sr: } \chi(r) = \sqrt{\frac{2}{\pi}} \kappa e^{-\kappa r}, \quad \text{Li: } \chi(r) = \sqrt{\frac{4}{3\pi}} \kappa'^2 r e^{-\kappa' r}, \quad (3)$$

with κ and κ' as variational parameters. Note that these solutions have s-wave symmetry. We have checked that the s-wave state is lower in energy than the p-wave one.

A variation of the energy (1) with respect to θ leads to,

$$\nabla^2\theta = \sqrt{2}g/\rho_s(\mathbf{e}\cdot\nabla)\chi^2(r),$$

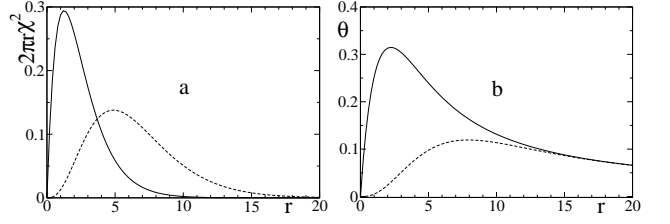


FIG. 1: **a:** The radial charge density $2\pi r\chi^2$ versus radius. **b:** The angle θ (radians) of the background spin rotation versus radius. The angle is given for direction $\mathbf{r}||\mathbf{e}$. The solid and the dashed lines correspond to Sr and Li impurities, respectively.

which has the solutions:

$$\begin{aligned} \text{Sr: } \theta &= \frac{g}{\sqrt{2}\pi\rho_s} \frac{(\mathbf{e}\cdot\mathbf{r})}{r^2} [1 - e^{-2\kappa r}(1 + 2\kappa r)], \\ \text{Li: } \theta &= \frac{g}{\sqrt{2}\pi\rho_s} \frac{(\mathbf{e}\cdot\mathbf{r})}{r^2} [1 - e^{-2\kappa' r}(1 + 2\kappa' r + 2\kappa'^2 r^2 + \frac{4}{3}\kappa'^3 r^3)]. \end{aligned} \quad (4)$$

Substitution of these solutions together with (2) and (3) in Eq. (1), and the minimization of energies with respect to κ and κ' leads to:

$$\begin{aligned} \text{Sr: } \kappa &= \frac{2e^2/(\epsilon_e\beta)}{\left(1 - \frac{g^2}{2\pi\beta\rho_s}\right)}, \quad E_{\text{Sr}} = -\frac{\beta\kappa^2}{2} \left(1 - \frac{g^2}{2\pi\beta\rho_s}\right), \\ \text{Li: } \kappa' &= \frac{2e^2/(\epsilon_e\beta)}{\left(1 - \frac{5g^2}{16\pi\beta\rho_s}\right)}, \quad E_{\text{Li}} = -\frac{\beta\kappa'^2}{6} \left(1 - \frac{5g^2}{16\pi\beta\rho_s}\right). \end{aligned} \quad (5)$$

The effective dielectric constant ϵ_e is not known accurately. Therefore, to determine κ we rely on the estimates that follow from the hopping conductivity [1, 15]: $\kappa \approx 0.4 \approx 0.1\text{\AA}^{-1}$. Then, from (5), one finds that $\kappa' \approx 0.31 \approx 0.08\text{\AA}^{-1}$, $E_{\text{Sr}}/J \approx -0.09$ (i.e., $E_{\text{Sr}} \approx -11$ meV), and $E_{\text{Li}}/J \approx -0.023$ (i.e., $E_{\text{Li}} \approx -3$ meV). Although the binding energies are subject to uncertainties associated with the value of the dielectric constant, the ratio $\kappa/\kappa' \approx 1.3$ and hence relative sizes of Sr and Li bound states are reliable. According to measurements [17] of the dielectric response of LCLiO, the charge excitation gap at $x = 0.023$ is $\Delta \approx 1$ meV. This value is in a reasonable agreement with our estimate $|E_{\text{Li}}| \approx 3$ meV especially having in mind that our result is relevant only to the very low doping, $x \ll 0.03$. We will argue below that the gap decreases with doping switching from one regime to another at $x \approx 0.03$.

Plots of radial charge density $2\pi r\chi^2(r)$ for Sr and Li impurities are given in Fig.1a. In Fig.1b we show the angle of the spin rotation of the antiferromagnetic background for Sr and Li impurities (see Eqs. (4)). Inside the “atomic core”, $r \ll 1/\kappa$, the Sr solution (4) describes a uniform $(1, \pm 1)$ spiral, $\theta \approx \sqrt{2}g\kappa^2(\mathbf{e}\cdot\mathbf{r})/(\pi\rho_s)$, while the Li solution (4) gives a very small rotation angle, $\theta \approx g\kappa'^4 r^2(\mathbf{e}\cdot\mathbf{r})/\rho_s$. This result indicates that while

Sr impurities induce incommensurate magnetic textures, Li impurities do not lead to a significant change in the commensurate state.

Destruction of the long-range order. According to Eq. (4), at large distances, $r \gg 1/\kappa$, the Sr and Li ions generate a similar disturbance in the antiferromagnetic background: $\delta \mathbf{n} = [\mathbf{n}_0 \times \mathbf{m}]\theta = \mathbf{M}(\mathbf{e} \cdot \mathbf{r})/(2\pi r^2)$, where $\mathbf{n} = \delta \mathbf{n} + \mathbf{n}_0$ is the Néel unit vector, $\mathbf{n}_0 = \mathbf{n}(r = \infty)$, and $|\mathbf{M}| = \sqrt{2}g/\rho_s \approx 8$ is the “dipole moment” of the bound state. It has been shown in Refs. [18, 19] that the dipoles frustrate the antiferromagnetism and hence lead to destruction of the Néel order at some critical concentration, x_c . Since M is more or less the same for LSCO and LCLiO, we would expect x_c to be the same in these two compounds. For $M \approx 8$ one finds $x_c \approx 0.02$ [11]. However, for $x \sim 0.02$ the average separation between ions is $r \sim 7a$ and hence, according to Fig.1b the effective dipole moment of the Li impurity is somewhat smaller than the one of Sr. Thus, the change in the dipole moment leads to a value of $x_c \approx 0.03$ for LCLiO that is slightly larger than the value of LSCO ($x_c \approx 0.02$). This result explains the destruction of Néel order in LCLiO.

In spite of similarity at very small x , the physics at $x > x_c$ in LSCO and LCLiO is quite different. It has been argued in Ref. [11] that for $0.02 < x < 0.055$ LSCO remains insulating because the bound states have not percolated. Nevertheless, because of the long-range dipole-dipole interaction between the bound states, the insulating spin-glass-like state with $(1, \pm 1)$ spiral ordering is established [20]. Due to the Dzyaloshinskii-Moriya interaction the spiral direction is pinned to the orthorhombic b-axis. The size of the Sr-hole bound state shown in Fig.1a is consistent with this picture. At $x \approx 0.055$ the Sr-hole bound states percolate and, due to the Pauli principle, there is a rotation of the spin spiral direction by 45° to the $(1,0)$ or $(0,1)$ incommensurate order [11]. At $x > 0.055$ the charge distribution is more homogeneous.

According to Fig.1a the size of the Li bound state is a factor 1.5 - 2 larger than that for Sr. Therefore in LCLiO there is no window of doping between destruction of the Néel order and percolation of bound states. Hence, percolation occurs at $x \approx x_c \approx 0.03$. However, after the percolation the system remains extremely inhomogeneous because of strong scattering of holes by Li ions. The hole localization length should be of the order of the mean free path that is of the order of the distance between impurities. Since the localization length is the same as the average separation between holes, the regions occupied by a single hole and regions occupied by two (or a few) holes are equally probable. It has been shown in Ref. [11] that single hole regions induce $(1, \pm 1)$ spirals while few hole regions induce $(1,0)$ or $(0,1)$ spirals. Thus, at any doping above the percolation the system remains completely frustrated and no collective spiral order can be established. The system consists of weakly and randomly coupled antiferromagnetic clusters. We call these

clusters antiferromagnetic shards.

This picture leads to a prediction for the nuclear quadrupole resonance (NQR) in LCLiO. It is known that in LSCO the Cu NQR A-line is shifted with respect to its position in the parent compound La_2CuO_4 , and the shift is proportional to doping [21]. The A-line is wide, reflecting a non-uniform charge distribution [22]. In the spin-shard state of LCLiO (i.e. at $x > 0.03$) one should expect two distinct NQR lines of comparable intensity (two Cu lines and two O-lines). The first one originates from antiferromagnetic shards. It is likely that the frequency of this line is close to that in the parent compound. The second line originates from regions occupied by holes and, therefore it should have a higher frequency and larger width. We note that inhomogeneities have already been observed in La-NQR in the ordered phase ($x < 0.025$) [23]. We assign those to the formation of bound states discussed here.

The spin-shard state. Below percolation, $x < x_c$ the system retains the long-range antiferromagnetic order. Above percolation, $x > x_c$ there are only finite antiferromagnetic shards with N spins because all exchange interactions are short range. In fact, there is a distribution of shard sizes and the probability of finding a shard of size N is given by percolation theory [24]:

$$P(N, x) \propto \exp\{-N/N(x)\}, \quad (6)$$

where $N(x)$ is the average shard size at doping x . Because of magnetic anisotropies in the system (Dzyaloshinskii-Moriya and crystal field) the low energy physics of the shard can be thought as a two-level system with a tunneling splitting, $\Delta(N)$, given by the WKB expression:

$$\Delta(N) \propto \omega_0 \exp\{-\gamma N\}, \quad (7)$$

where $\omega_0 \propto J$ is an attempting frequency and γ is a parameter that depends on the magnetic anisotropies. The combination of (6) and (7) shows that there is a distribution of tunneling splittings in the problem that has the form:

$$P(\Delta) \propto \Delta^{\alpha-1},$$

where $\alpha = 1/(\gamma N(x))$ is a non-universal quantity which depends on doping. The neutron scattering is peaked at $\mathbf{q} = (\pi, \pi)$, and the imaginary part of the average susceptibility is given by:

$$\chi''_{\mu}(\omega, B, T) = \int d\Delta P(\Delta) \chi''_{\mu, \text{shard}}(\omega, B, T, \Delta), \quad (8)$$

where $\mu = 0, 1$ refers respectively to longitudinal and transverse polarizations of the neutron magnetic field with respect to the applied uniform external magnetic field B . The shard susceptibility is given by the two-level

system expression ($\omega > 0$):

$$\chi''_{\mu, \text{shard}} \propto \frac{(\Delta^2)^{1-\mu} (\mathcal{M}^2)^\mu}{\Delta^2 + \mathcal{M}^2} \tanh\left(\frac{\sqrt{\mathcal{M}^2 + \Delta^2}}{2T}\right) \delta(\omega - \sqrt{\mathcal{M}^2 + \Delta^2}),$$

where $\mathcal{M}(B) \propto \mu_B \sqrt{N} B$ is the Zeeman energy (since a shard of N spins is a random system, there are on average \sqrt{N} more spins in one sublattice than in the other leading to a net shard moment). Hence, the integration in (8) gives the following result:

$$\chi''_{\mu}(\omega, B, T) = \frac{1}{T^{1-\alpha}} F_{\mu}(\omega/T, \mathcal{M}/\omega), \quad (9)$$

where

$$F_{\mu}(x, y) \propto x^{\alpha-1} y^{2\mu} (1 - y^2)^{\alpha/2-\mu} \tanh(x/2) \Theta(1 - y)$$

is a scaling function [25], where $\Theta(x) = 1(0)$ if $x > 0$ ($x < 0$) is the Heaviside step function. In a unpolarized neutron scattering experiment both longitudinal and transverse responses appear. When $y \sim 1$, as in the case of nuclear magnetic resonance (NMR) [26], the transverse response is the dominant one. In this case, since we expect $\alpha < 1$, the transverse susceptibility ($\mu = 1$) becomes singular at $y = 1$ while the longitudinal response ($\mu = 0$) vanishes. This resonant effect should be easily observable in neutron scattering experiments in a finite magnetic field because the damping to the shard motion should be weak due to the insulating nature of the background. Equation (9) is in agreement with zero magnetic field ($\mu = 0, y \rightarrow 0$) experimental data of Ref. [8] with $\alpha \approx 0.35$ for $x = 0.04$ and $\alpha \approx 0.06$ for $x = 0.06$ and $x = 0.1$. By performing the same experiments in a magnetic field one can test our prediction for (9).

In reality the antiferromagnetic shards are not decoupled. Shards from different CuO_2 planes interact because of the interplane exchange J_{\perp} . Due to this interaction the system must freeze to a disordered 3D spin-shard glass at the characteristic temperature $T_{3D} \sim J_{\perp} N_{ov}$, where $N_{ov} \sim N(x)$ is the number of spins in two shards that overlap along the c -axis. Thus, Eq. (9) is relevant to the spin-shard state at $T > T_{3D}$ where shards fluctuate independently. At $T < T_{3D}$ the shards freeze. However, Eq. (9) is still valid, but instead of the current temperature T one must substitute the freezing temperature T_{3D} . Thus, for $T < T_{3D}$ one finds that $\chi''(\omega, T)$ should be roughly temperature independent, in agreement with the experimental data [8, 9].

In conclusion, based on an analysis of the extended $t - J$ model, we propose the theory of antiferromagnetic spin-shard state for $\text{La}_2\text{Cu}_{1-x}\text{Li}_x\text{O}_4$. The theory explains why the long-range Néel order is destroyed at $x_c = 0.03$. At $x < x_c$ physics of the system is driven by Li-hole bound states. At $x = x_c$ the Néel order is destroyed and simultaneously the bound states percolate.

At $x > x_c$ the holes in $\text{La}_2\text{Cu}_{1-x}\text{Li}_x\text{O}_4$ remain localized breaking the global antiferromagnetic state into array of weakly coupled 2D antiferromagnetic shards. Due to the interlayer interaction the shard state freezes to a glassy state (spin-shard-glass) below some characteristic temperature T_{3D} . While our theory describes quite well the available experimental data, it also predicts two independent effects: the existence of two distinct $\text{Cu}(\text{O})$ -NQR lines, and a magnetic field scaling of the neutron scattering data.

We would like to thank Wei Bao, Anders Sandvik, and John Sarrao for stimulating discussions. O.P.S. acknowledges the Quantum Condensed Matter Visitor's Program at Boston University, and the Kavli Institute for Theoretical Physics at UCSB (support by the NSF Grant No. PHY99-07949) for their hospitality. A.H.C.N. was supported through NSF grant DMR-0343790.

-
- [1] See review M. A. Kastner *et al.*, Rev. Mod. Phys., **70**, 897 (1998).
 - [2] J. L. Sarrao *et al.*, Phys. Rev. B **54**, 12014 (1996).
 - [3] K. Yamada *et al.*, Phys. Rev. B **57**, 6165 (1998).
 - [4] S. Wakimoto *et al.*, Phys. Rev. B **60**, R769 (1999).
 - [5] M. Matsuda *et al.*, Phys. Rev. B **62**, 9148 (2000).
 - [6] M. Fujita *et al.*, Phys. Rev. B **65**, 064505 (2002).
 - [7] Wei Bao *et al.*, Phys. Rev. Lett. **84**, 3978 (2000).
 - [8] Y. Chen *et al.*, cond-mat/0408547.
 - [9] Y. Chen *et al.*, cond-mat/0503167.
 - [10] R. H. Heffner *et al.*, Physica B **312-313**, 65 (2002).
 - [11] O. P. Sushkov and V. N. Kotov, Phys. Rev. Lett., **94**, 097005 (2005).
 - [12] Y. Tokura *et al.*, Phys. Rev. B **41**, 11657 (1990).
 - [13] O. K. Andersen, A. I. Liechtenstein, O. Jepsen, and F. Paulsen, J. Phys. Chem. Solids **56**, 1573 (1995); E. Pavarini *et al.*, Phys. Rev. Lett. **87**, 047003 (2001).
 - [14] The matrix elements t' and t'' are *qualitatively* important for stability of the superconducting phase of $\text{La}_{2-x}\text{Sr}_x\text{CuO}_4$ at $x > 0.055$, see Ref. [15].
 - [15] O. P. Sushkov and V. N. Kotov, Phys. Rev. B **70**, 024503 (2004); V. N. Kotov and O. P. Sushkov, Phys. Rev. B **70**, 195105 (2004).
 - [16] J. Igarashi and P. Fulde, Phys. Rev. B **45**, 10419 (1992).
 - [17] Tuson Park *et al.*, Phys. Rev. Lett. **94**, 017002 (2005).
 - [18] L. I. Glazman and A. S. Ioselevich, Z. Phys. B **80**, 133 (1990).
 - [19] V. Cherepanov, I. Ya. Korenblit, A. Aharony, and O. Entin-Wohlman, Eur. Phys. J. B **8**, 511 (1999).
 - [20] N. Hasselmann, A. H. Castro Neto, and C. Morais Smith, Phys. Rev. B **69**, 014424 (2004).
 - [21] S. Ohsugi *et al.*, J. Phys. Soc. Jpn. **63**, 700 (1994).
 - [22] J. Haase *et al.*, Phys. Rev. B **69**, 094504 (2004).
 - [23] B. J. Suh *et al.*, Phys. Rev. Lett. **81**, 2791 (1998).
 - [24] D. Stauffer and A. Aharony, *Introduction to Percolation Theory* (Taylor & Francis, London, 2001).
 - [25] In writing (9) we have disregarded logarithmic corrections.
 - [26] A. Abragam, *The principles of Nuclear Magnetism* (Clarendon Press, Oxford, 1961).